

Hetero-multimetallic Tetrakis(SCS-pincer palladium)–(Metallo)porphyrin Hybrids. Tunable Precatalysts in a Heck Reaction

Bart M. J. M. Suijkerbuijk, Sara D. Herreras Martínez, Gerard van Koten, and Robertus J. M. Klein Gebbink*

Chemical Biology & Organic Chemistry, Department of Chemistry, Faculty of Science, Utrecht University, Padualaan 8, 3584 CH Utrecht, The Netherlands

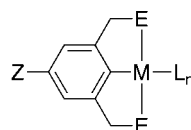
Received June 8, 2007

A series of *meso*-tetrakis(SCS-pincer PdCl)–(metallo)porphyrin hybrids have been synthesized using two distinct synthetic routes. Manganese and nickel were introduced into the porphyrin macrocycle prior to peripheral electrophilic palladation, whereas magnesium was introduced thereafter in light of its acid sensitivity. When these complexes were used as precatalysts in the Heck reaction between iodobenzene and styrene, different catalytic activities were observed for each hybrid complex. The catalytic activity increased for the metalloporphyrin series $\text{MnCl} < 2\text{H} < \text{Ni} < \text{Mg}$, which interestingly coincides with an increase of electron richness of the porphyrin ring. Control experiments on model compounds confirmed that an intramolecular effect rather than an intermolecular effect was responsible for this influence. We postulate that, in analogy with related NCN-pincer metal complexes, the electron density on the palladium atom in SCS-pincer palladium complexes is influenced by the electronic properties of the *para*-substituent, i.e., the metalloporphyrin in this case. This in turn influences the rate of palladium leaching and, hence, of catalysis.

Introduction

ECE-pincer complexes of a multitude of transition metals (Chart 1) have taken center stage as one of the most promising classes of organometallic complexes, a fact that is largely attributable to the impressive scope of their applications combined with their facile synthesis.^{1–3} Another factor contributing to the popularity of these complexes is the ease with which their reactivity can be modulated through modification of several key features, viz., the metal M, the benzylic donor atoms E, and the ligand(s) L. In this regard, especially the palladium(II) complexes of the 2,6-bis[(phenylsulfido)methyl]phen-1-yl (SCS-pincer) ligands have enjoyed widespread attention. Loeb,^{4,5} Reinhoudt,^{6–8} and Weck^{9–12} have explored their use for the

Chart 1. General Formula of ECE-Pincer Metal Complexes



M = Li, Rh, Ru, Ni, Pd, Pt, Au
 E = NR₂, OR, PR₂, SR, SeR
 L = Lewis base, halide
 n = 1, 2, 3
 Z = *para*-substituent

construction of supramolecular architectures, using the fourth ligand position L for the attachment of functionalized Lewis bases. Moreover, continuing research addresses their ability to act as precatalysts for high-temperature palladium-catalyzed organic transformations, particularly Heck reactions.^{13–20}

For most of its applications, the *para*-substituent Z of SCS-pincer palladium complexes has been utilized to immobilize this moiety onto larger fragments, specifically for catalytic reuse.^{21–24} For these systems, the electronic influence exerted by the *para*-substituent on the chelated palladium center has received little attention, whereas the relationship between the electronic properties of the pincer *para*-substituent Z and the electron

* r.j.m.kleingebink@uu.nl, Phone: +31-30-2531889; Fax: +31-30-2523615.

(1) Albrecht, M.; van Koten, G. *Angew. Chem., Int. Ed.* **2001**, *40*, 3750–3781.

(2) Singleton, J. T. *Tetrahedron* **2003**, *59*, 1837–1857.

(3) van der Boom, M. E.; Milstein, D. *Chem. Rev.* **2003**, *103*, 1759–1792.

(4) Hall, J. R.; Loeb, S. J.; Shimizu, G. K. H.; Yap, G. P. A. *Angew. Chem., Int. Ed.* **1998**, *37*, 121–123.

(5) Kickham, J. E.; Loeb, S. J.; Murphy, S. L. *Chem. Eur. J.* **1997**, *3*, 1203–1213.

(6) Huck, W. T. S.; Prins, L. J.; Fokkens, R. H.; Nibbering, N. M. M.; van Veggel, F. C. J. M.; Reinhoudt, D. N. *J. Am. Chem. Soc.* **1998**, *120*, 6240–6246.

(7) Huck, W. T. S.; van Veggel, F. C. J. M.; Kropman, B. L.; Blank, D. H. A.; Keim, E. G.; Smithers, M. M. A.; Reinhoudt, D. N. *J. Am. Chem. Soc.* **1995**, *117*, 8293–8294.

(8) Huck, W. T. S.; van Veggel, F. C. J. M.; Reinhoudt, D. N. *Angew. Chem., Int. Ed. Engl.* **1996**, *35*, 1213–1215.

(9) Pollino, J. M.; Stubbs, L. P.; Weck, M. *Macromolecules* **2003**, *36*, 2230–2234.

(10) Pollino, J. M.; Stubbs, L. P.; Weck, M. *J. Am. Chem. Soc.* **2004**, *126*, 563–567.

(11) Pollino, J. M.; Weck, M. *Synthesis* **2002**, 1277, 1285.

(12) Pollino, J. M.; Weck, M. *Chem. Soc. Rev.* **2005**, *34*, 193–207.

(13) Bergbreiter, D. E.; Osburn, P. L.; Liu, Y.-S. *J. Am. Chem. Soc.* **1999**, *121*, 9531–9538.

(14) Beletskaya, I. P.; Cheprakov, A. V. *J. Organomet. Chem.* **2004**, *689*, 4055–4082.

(15) Bergbreiter, D. E.; Osburn, P. L.; Frels, J. D. *Adv. Synth. Catal.* **2005**, *347*, 172–184.

(16) Sommer, W.; Yu, K.; Sears, J. S.; Ji, Y.; Zheng, X.; Davis, R. J.; Sherrill, C. D.; Jones, C. W.; Weck, M. *Organometallics* **2005**, *24*, 4351–4361.

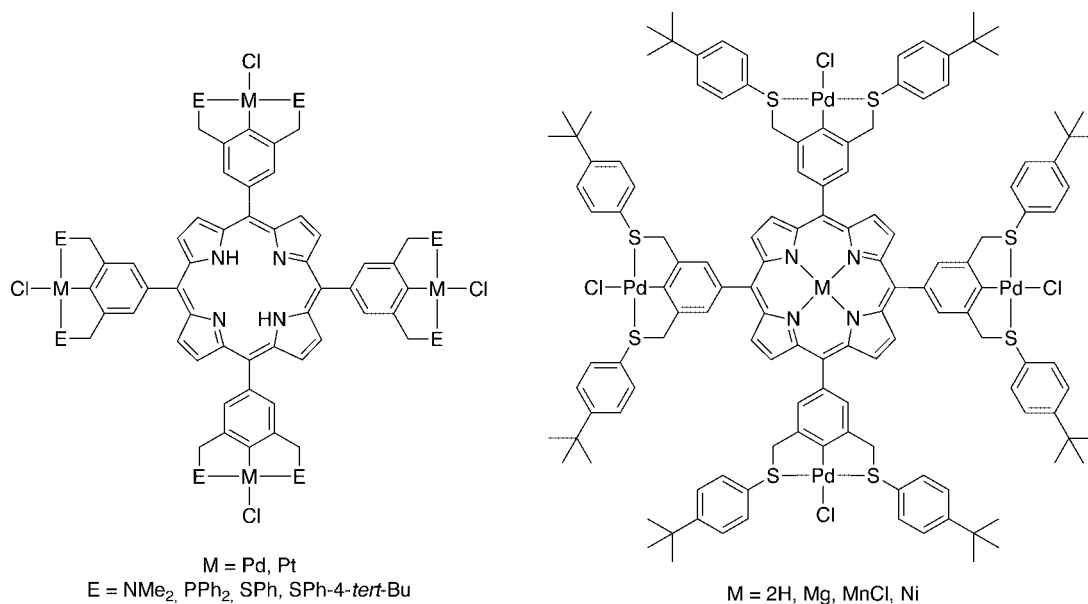
(17) Yu, K.; Sommer, W.; Richardson, J. M.; Weck, M.; Jones, C. W. *Adv. Synth. Catal.* **2005**, *347*, 161–171.

(18) Bergbreiter, D. E.; Li, J. *Chem. Commun.* **2004**, 42–43.

(19) Bergbreiter, D. E.; Osburn, P. L.; Frels, J. D. *J. Am. Chem. Soc.* **2001**, *123*, 11105–11106.

(20) Bergbreiter, D. E.; Osburn, P. L.; Wilson, A.; Sink, E. M. *J. Am. Chem. Soc.* **2000**, *122*, 9058–9064.

Chart 2. General Formula of Peripherally Metalated Pincer-Porphyrin Hybrids



density on the metal (and thus its reactivity) has been well established for similar pincer metal complexes.^{25–30}

We recently reported on the synthesis of a number of peripherally metalated pincer-porphyrin hybrids (Chart 2, left) and showed that the introduction of metal sites at the porphyrin's periphery has a substantial effect on the electronic absorption spectrum and emission properties of the porphyrin core.^{31,32} Since the metalated pincer groups affect the physical characteristics of the porphyrin core, we set out to investigate the reciprocal effect, i.e., the influence of the porphyrin core on the properties of the peripheral ECE-pincer metal groups. It was found that in *meso*-(NCN-pincer PtCl)-(metallo)porphyrin hybrids the electron density at the peripheral NCN-pincer Pt centers depends on the electronic properties of the (metallo)porphyrin.^{32,33} Interestingly, the electronic properties of the porphyrin can be modified by complexation of a metal in the central

N₄²⁻ coordination cavity.^{34–36} Virtually all metals can be introduced in the porphyrin system using mild procedures, and this provides a possible handle for remote, yet intramolecular, control over the properties of the peripheral organometallic groups. In other words, the free-base porphyrin can potentially act as a modular *para*-substituent precursor.

In the investigations reported here, it was decided to focus on *meso*-tetrakis(SCS-pincer Pd)-(metallo)porphyrin hybrids and to investigate the effects of the (metallo)porphyrin on the peripheral palladium moieties. In order to maximize the observable effects, the porphyrin was metalated with metals ranging from electropositive Mg(II) to electronegative Mn(III) to give a novel class of heteromultimetallic pincer-porphyrin hybrids (Chart 2, right). The intramolecular effects were probed by applying these complexes as catalyst precursors in the Heck reaction of iodobenzene with styrene, since it has been pointed out that different palladacycles lead to different catalytic activities.³⁷

Results

Synthesis and Characterization. All heteromultimetallic target compounds were synthesized from the previously reported *meso*-tetrakis(3,5-bis[(4-*tert*-butylphenyl)sulfido)methyl]phenyl)porphyrin **1(2H)**,³¹ which comprises four SCS-pincer ligand groups connected to a porphyrin core via its four *meso*-positions. The *tert*-butyl groups at the thiophenyl substituents serve as solubilizing groups, since the parent tetrakis(SCS-pincer)porphyrin is too insoluble for subsequent reactions.³¹ Depending on the targeted *meso*-tetrakis(SCS-pincer PdCl)-(metallo)porphyrin hybrid complex, two distinct metalation strategies were employed (see Scheme 1). Route A comprises metalation of the tetrapyrrolic macrocycle followed by peripheral palladation of the SCS-pincer moieties, while in route B the pincer ligands are metalated prior to the central porphyrin ring.

(21) Dijkstra, H. P.; Meijer, M. D.; Patel, J.; Kreiter, R.; van Klink, G. P. M.; Lutz, M.; Spek, A. L.; Canty, A. J.; van Koten, G. *Organometallics* **2001**, *20*, 3159–3168.

(22) Dijkstra, H. P.; Steenwinkel, P.; Grove, D. M.; Lutz, M.; Spek, A. L.; van Koten, G. *Angew. Chem., Int. Ed.* **1999**, *38*, 2186–2187.

(23) Gimenez, R.; Swager, T. J. *Mol. Catal. A: Chem.* **2001**, *166*, 265–273.

(24) Bergbreiter, D. E.; Sung, S. D. *Adv. Synth. Catal.* **2006**, *348*, 1352–1366.

(25) Dijkstra, H. P.; Slagt, M. Q.; McDonald, A.; Kruihof, C. A.; Kreiter, R.; Mills, A. M.; Lutz, M.; Spek, A. L.; Klopper, W.; van Klink, G. P. M.; van Koten, G. *Eur. J. Inorg. Chem.* **2003**, 830–838.

(26) Slagt, M. Q.; Rodríguez, G.; Grutters, M. M. P.; Klein Gebbink, R. J. M.; Klopper, W.; Jenneskens, L. W.; Lutz, M.; Spek, A. L.; van Koten, G. *Chem. Eur. J.* **2004**, *10*, 1331–1344.

(27) Tromp, M.; van Bokhoven, J. A.; Slagt, M. Q.; Klein Gebbink, R. J. M.; van Koten, G.; Ramaker, D. E.; Koningsberger, D. C. *J. Am. Chem. Soc.* **2004**, *126*, 4090–4091.

(28) van de Kuil, L. A.; Luitjes, H.; Grove, D. M.; Zwikker, J. W.; van der Linden, J. G. M.; Roelofsens, A. M.; Jenneskens, L. W.; Drenth, W.; van Koten, G. *Organometallics* **1994**, *13*, 468–477.

(29) Aydin, J.; Selander, N.; Szabó, *Tetrahedron Lett.* **2007**, *47*, 8999–9001.

(30) Fossey, J. S.; Richards, C. J. *Organometallics* **2004**, *23*, 367–373.

(31) Suijkerbuijk, B. M. J. M.; Lutz, M.; Spek, A. L.; van Koten, G.; Klein Gebbink, R. J. M. *Org. Lett.* **2004**, *6*, 3023–3026.

(32) Suijkerbuijk, B. M. J. M.; Tooke, D. M.; Lutz, M.; Spek, A. L.; van Koten, G.; Klein Gebbink, R. J. M. Manuscript in preparation.

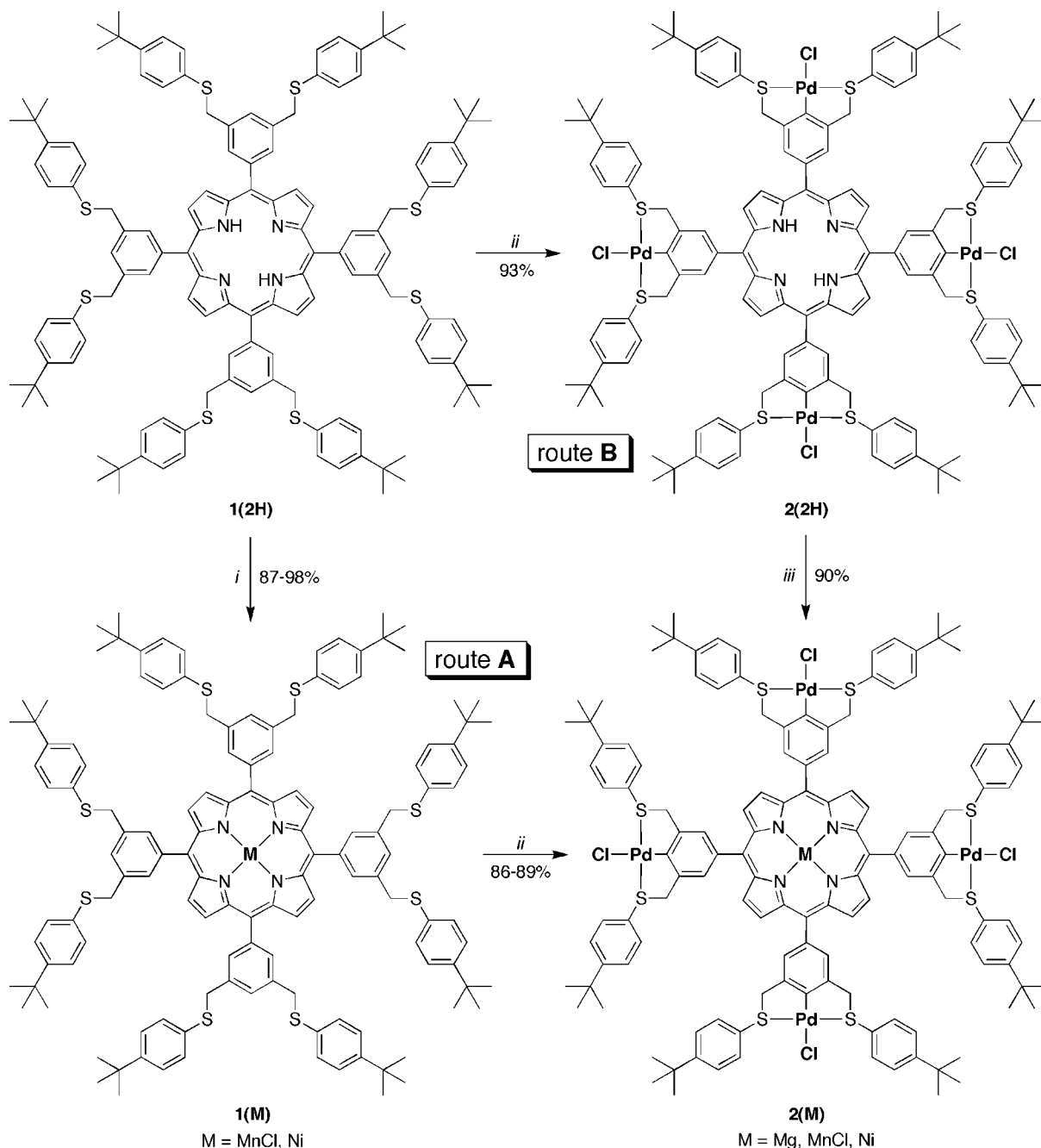
(33) Suijkerbuijk, B. M. J. M.; Schamhart, D. J.; Kooijman, H.; Spek, A. L.; van Koten, G.; Klein Gebbink, R. J. M. Manuscript in preparation.

(34) Dolphin, D. *The Porphyrins*; Academic Press, Inc.: New York, 1978.

(35) Smith, K. M., *Porphyrins and Metalloporphyrins*; Elsevier Scientific Publishing Company: Amsterdam, 1975.

(36) Liao, M.-S.; Scheiner, S. *J. Chem. Phys.* **2002**, *117*, 205–219.

(37) Phan, N. T. S.; Van Der Sluys, M.; Jones, C. W. *Adv. Synth. Catal.* **2006**, *348*, 609–679.

Scheme 1. Synthetic Route towards *meso*-Tetrakis(SCS-pincer PdCl)–Metalloporphyrin Hybrids^a

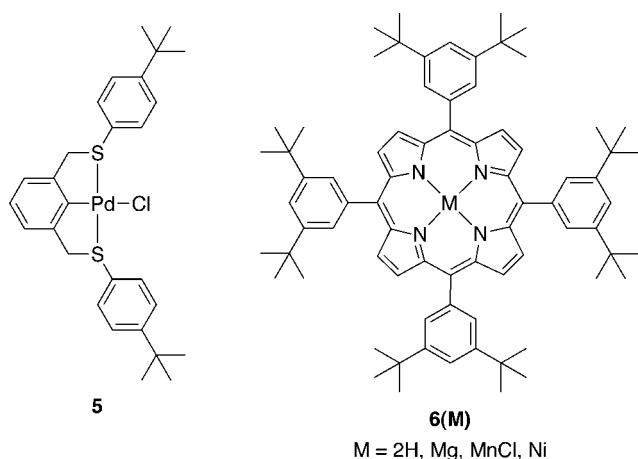
^a (i) for M = MnCl: (a) Mn(OAc)₂·4H₂O, DMF, Δ; (b) NaCl, H₂O/CH₂Cl₂; for M = Ni: Ni(acac)₂, toluene, Δ; (ii) (a) [Pd(NCMe)₄](BF₄)₂, MeCN/CH₂Cl₂, Δ; (b) LiCl, MeCN; (iii) MgBr₂·OEt₂, Et₃N, CH₂Cl₂.

Mn(III) and Ni(II) were readily introduced in the porphyrin core of **1(2H)** via reaction with Mn(OAc)₂·4H₂O and Ni(acac)₂, respectively, to give **1(MnCl)** and **1(Ni)** in good yields. Although Mn(III) insertion is usually performed under aerobic conditions to oxidize the initially formed Mn(II) porphyrin,³⁵ a slightly modified procedure was used in this case. In light of the substantial susceptibility of the sulfur atoms of **1(2H)** toward oxidation, a brief exposure to air (30 s) in the presence of NaCl at room temperature was used instead after completion of the Mn(II) insertion to successfully generate **1(MnCl)** in 87% yield. Porphyrin **1(Ni)** was synthesized in 98% yield by reaction of **1(2H)** with 20 equiv of Ni(acac)₂ in boiling toluene.

Subsequently, the SCS-pincer ligand moieties of metalloporphyrins **1(MnCl)** and **1(Ni)** were selectively palladated with [Pd(NCMe)₄](BF₄)₂ in a mixture of CH₂Cl₂ and MeCN.⁶

The resulting tetracationic species were converted into the corresponding tetrachloride complexes with an excess of LiCl to give **2(MnCl)** and **2(Ni)** in 86% and 89%, respectively. For the synthesis of **2(Mg)**, however, this approach gave problems since magnesium(II) porphyrins are highly unstable toward acidic conditions.³⁵ When an SCS-pincer ligand was treated with [Pd(NCMe)₄](BF₄)₂ in the presence of a magnesium porphyrin (**6(Mg)**, see Chart 3), the porphyrin was quickly demetallated by HBF₄ generated during the electrophilic palladation. This precluded the use of route A for the synthesis of multimetallic porphyrin **2(Mg)**, which was therefore synthesized via route B.

Upon treatment of **1(2H)** with 4 equiv of [Pd(NCMe)₄](BF₄)₂ in a CH₂Cl₂/MeCN mixture, a fast color change from deep red via brown to deep green was observed. The deep red color of

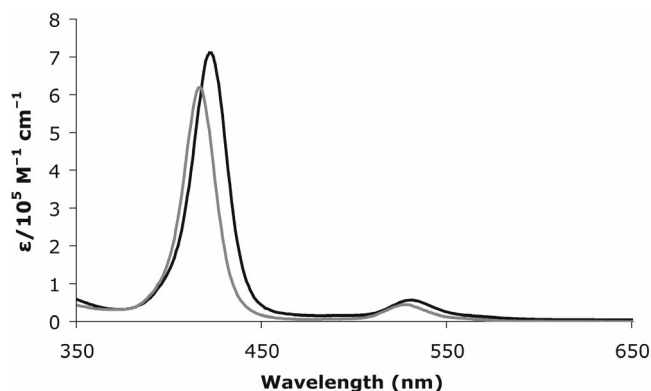
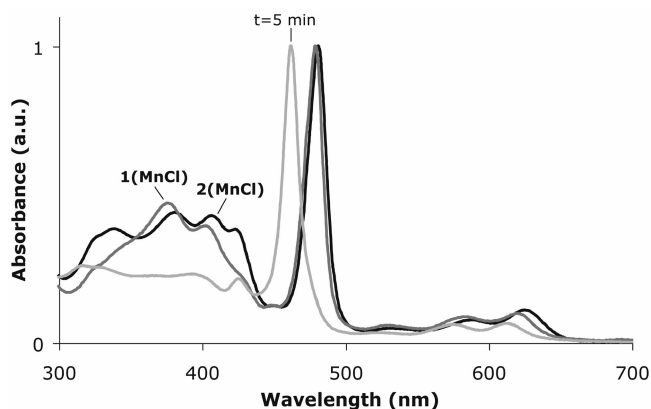
Chart 3. Structural Formulas of Model SCS-Pincer Palladium Compound **5 and Reference Metalloporphyrins **6(M)****

the free-base porphyrin was regenerated by addition of an excess of Et_3N , which indicated that the porphyrin dication, formed by protonation of the free-base porphyrin by HBF_4 , which is liberated during the electrophilic palladation reaction, was responsible for the green color. The tetracationic SCS-pincer palladium(II) porphyrin was subsequently treated with an excess of LiCl in MeCN to give the desired complex **2(2H)** in 93% yield. The selectivity of this reaction for the peripheral SCS-pincer ligand sites was confirmed by ^1H NMR spectroscopy, which showed similar ratios between the integrals corresponding to the benzylic and pyrrolic protons, respectively, of **1(2H)** ($\delta = 4.30$ (s) and -3.00 ppm, respectively) and **2(2H)** ($\delta = 4.83$ (br) and -2.86 ppm, respectively; for an X-ray crystal structure of **2(2H)** see Supporting Information, Figure S1). It was observed that after peripheral palladation, i.e., coordination of the sulfur atoms to palladium, the compounds were stable toward oxidation and could be stored under air for several months. Free-base porphyrin **2(2H)** was then reacted with $\text{MgBr}_2 \cdot \text{OEt}_2$ in the presence of Et_3N^{38} to give **2(Mg)** in 90% yield. Route B could not be employed to synthesize **2(MnCl)**, since **2(2H)** was not stable under the rather forcing conditions of Mn(III) insertion (refluxing DMF, vide supra). Divalent nickel could be inserted into **2(2H)** using $\text{Ni}(\text{OAc})_2$ in a mixed solvent system ($\text{MeOH}/\text{CH}_2\text{Cl}_2$), but the isolated yields were generally low ($\sim 60\%$).

For reasons of comparison, 2,6-bis[(4-*tert*-butylphenyl)sulfido)methyl]-1-chloridopalladio(II)benzene (**5**) and *meso*-tetrakis[3,5-bis(*tert*-butyl)phenyl]porphyrin (**6(2H)**) and its corresponding metal complexes (**6(M)**; M = Mg, MnCl, Ni) were synthesized (Chart 3). All compounds were fully characterized by means of ^1H and $^{13}\text{C}\{^1\text{H}\}$ NMR spectroscopy, UV/vis spectroscopy, mass spectrometry, and elemental analysis (see Supporting Information).

UV/Vis Spectroscopy. The UV/vis spectra of **1(M)** are dominated by the features of the (metallo)porphyrin core, whose molar absorption coefficients exceed those of the SCS-pincer ligand moieties by 2 orders of magnitude. When **1(Ni)** was treated with $[\text{Pd}(\text{NCMe})_4](\text{BF}_4)_2$, a fast color change (orange to darker red) of the reaction mixture occurred, which, over time, gradually returned to the original color. After workup of the reaction, the Soret and Q-band of **2(Ni)** had shifted bathochromically by 6 nm with respect to the parent **1(Ni)**, and the molar absorption coefficient ϵ of each band had increased (Figure 1).

The spectral changes during palladation of **1(MnCl)** are shown in Figure 2. Five minutes after addition of $[\text{Pd}$

**Figure 1.** Comparison of the Soret and Q-band region of the electronic spectra of **1(Ni)** (gray) and **2(Ni)** (black).**Figure 2.** Evolution of the normalized electronic spectra of the reaction between **1(MnCl)** and $[\text{Pd}(\text{NCMe})_4](\text{BF}_4)_2$.**Table 1. Positions of Peak Maxima of **1(M)** and **2(M)** in nm**

M	Soret band (log ϵ) 1(M)	Soret band (log ϵ) 2(M)
2H	420 (5.73)	426 (5.79)
Mg	n/a	433 (5.82)
MnCl	479 (5.14)	481 (5.20)
Ni	417 (5.79)	422 (5.85)

$(\text{NCMe})_4](\text{BF}_4)_2$ a spectrum was recorded in which the Soret band has shifted hypsochromically from 479 to 462 nm. During the course of the reaction the Soret band gradually shifted bathochromically to 481 nm for the product **2(MnCl)**.

These observations might be attributed to the electronic effects exerted by the intermediates of the palladation reaction on the porphyrin core. It is known that during an electrophilic palladation of an ECE-pincer ligand ($\text{E} = \text{NR}_2, \text{SR}, \text{PR}_2$) a positively charged arenium ion is initially formed.^{39–41} In the present *meso*-tetrakis(SCS-pincer)–(metallo)porphyrin hybrids, this means that in total four arenium ions initially develop at the *meso*-phenyl positions of the porphyrin. These render the *meso*-groups relatively electron-poor, which in turn has an electron-withdrawing effect on the porphyrin ring. This leads to a reduction of the electron density on the latter and induces a hypsochromic shift of the Soret band.⁴² As the reaction

(39) Canty, A. J.; van Koten, G. *Acc. Chem. Res.* **1995**, *28*, 406–413.(40) Ryabov, A. D. *Chem. Rev.* **1990**, *90*, 403–424.(41) Davies, D. L.; Donald, S. M. A.; Macgregor, S. A. *J. Am. Chem. Soc.* **2005**, *127*, 13754–13755.(42) Foran, G. J.; Armstrong, R. S.; Crossley, M. J.; Lay, P. A. *Inorg. Chem.* **1992**, *31*, 1463–1470.(38) Lindsey, J. S.; Woodford, J. N. *Inorg. Chem.* **1995**, *34*, 1063–1069.

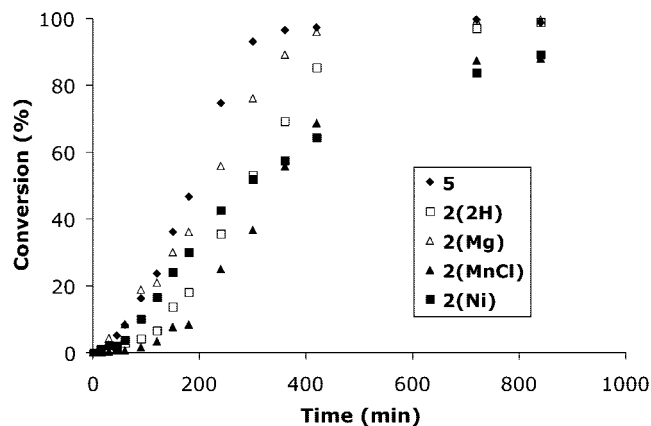
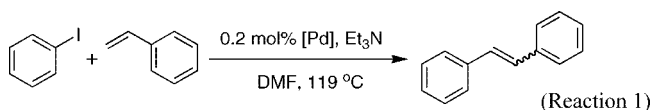


Figure 3. Plot of the conversion of starting materials to styrene products vs time for reaction 1, catalyzed by **5** and several tetrakis(SCS-pincer PdCl)–(metallo)porphyrin hybrids.

proceeds, H^+ is eliminated from the *meso*-arenium groups to form the *meso*-[3,5-bis([4-*tert*-butylphenylsulfido)methyl]-4-palladium(II)] $^+$ groups. After workup, the spectrum of **2(MnCl)** exhibited similar features compared to that of **1(MnCl)**, albeit with small bathochromic shifts (Figure 2).

The Soret band wavelengths and molar absorption coefficients of **1(M)** and **2(M)** are listed in Table 1. Important to note is that the peak maxima of all compounds show a similar bathochromic shift, with a concomitant increase of ϵ . The bathochromic shifts caused by palladation of the peripheral SCS-pincer ligand groups might be attributed to the electron-releasing nature of Pd when σ -bonded to an aryl fragment.^{26,43} The palladium-induced higher electron density on the *meso*-aryl groups of **2(M)** may lead to a decreased HOMO–LUMO gap, which results in a red-shift of the electronic absorption bands of **2(M)** compared to **1(M)**. A similar phenomenon was observed for the structurally related *meso*-tetrakis(NCN-pincer MX)–(metallo)porphyrin hybrids (MX = PdBr, PtCl).³²

Catalysis. With compounds **2(M)** in hand, their behavior as precatalysts for the Heck reaction between iodobenzene and styrene was investigated (reaction 1). The catalytic experiments were conducted in DMF at 119 °C with 1 equiv of iodobenzene, 1.5 equiv of styrene, 1.5 equiv of Et_3N , and 0.2 mol % of the Pd-catalyst, i.e., with 0.05 mol % of the respective pincer-porphyrin hybrid **2(M)**. Each experiment was run three times to ensure reproducibility of the results.



For the pincer–porphyrin hybrids **2(M)** different plots were found for the conversion versus time (see Figure 3). All traces showed a sigmoidal curve with an induction period, which is consistent with the kinetic data obtained for other ECE-pincer PdCl-catalyzed Heck reactions in the literature.^{10,15–17} The parent SCS-pincer PdCl complex **5** was found to be the most active with the shortest induction period. For the pincer–porphyrin hybrids, the induction times increased in the order **2(Mg)** < **2(Ni)** < **2(2H)** < **2(MnCl)**. Interestingly, this order coincides with the order of decreasing HOMO energy of the metallo(porphyrin) macrocycle.⁴⁴ After 240 min of reaction, complex **5**

gave 75% conversion, while the most active pincer–porphyrin catalyst precursor **2(Mg)** exhibited 56% conversion at the same time. By that time the other pincer–porphyrin hybrids catalyst precursors had converted considerably smaller amounts of starting materials, with **2(MnCl)** being the least active at 24% conversion. A conversion of >95% was reached first by **5** (6 h) followed by **2(Mg)** and **2(2H)** (7 h and approximately 10 h, respectively). After a relatively short induction period, the reaction catalyzed by **2(Ni)** had slowed down to give 90% conversion after 14 h, requiring 25 h to reach full conversion. The relatively electron-poor manganese(III) porphyrin **2(MnCl)** exhibited the least activity (92% conversion after 45 h).

Since possible differences between the catalytic behavior among the tetrakis(SCS-pincer PdCl)–(metallo)porphyrin hybrids **2(M)** might have originated from *intermolecular* processes rather than *intramolecular* processes, we conducted some systematic catalytic studies on appropriate combinations of their components, i.e., 4 equiv of **5** and 1 equiv of the respective model (metallo)porphyrin **6(M)**. These experiments showed that all mixtures of precatalysts led to virtually identical product yields and kinetic traces (analogous to that of **5**), and it was thus concluded that intermolecular interactions between the palladacycles and (metallo)porphyrins did not affect the catalytic behavior of the systems. Control experiments with the metalloporphyrins **6(M)** furthermore showed that these (metallo)porphyrins did not exhibit any reactivity in the same Heck reaction. These results indicate that the differences in catalytic activity among the multimetallic pincer–porphyrin hybrids **2(M)** arise from *intramolecular* interactions within the pincer–porphyrin hybrids and not from *intermolecular* interactions between individual molecules.

As Figure 3 shows, the reactions catalyzed by precatalysts **5** and **2(M)** all exhibit sigmoidal kinetics. As was recently shown by the group of Weck,¹⁷ the sigmoidal curves observed from SCS-pincer PdCl-catalyzed Heck reactions can be fitted to a modified version of Finke's model for transition metal nanoparticle formation.^{45,46} In this model, a key notion is that the rate of product formation will follow the kinetic model for metal-particle formation. According to Finke's model, the formation of nanoparticles can be modeled using the combination of a nucleation step (SCS-pincer PdCl \rightarrow Pd(0), with rate constant k_1) and an autocatalytic surface growth step (Pd(0) + SCS-pincer PdCl \rightarrow 2 Pd(0), with rate constant k_2). If the actual stoichiometric catalytic cycle, i.e., Pd(0) + styrene + iodobenzene \rightarrow Pd(0) + stilbene + HI, with rate constant k_3 , is then assumed to be fast relative to k_1 and k_2 , it follows that the kinetics of the overall reaction are those of the first two steps. The following expression (eq 1) is then obtained for the concentration of SCS-pincer PdCl ($[A]$) in time:⁴⁶

$$[A]_t = \frac{\frac{k_1}{k_2} + [A]_0}{1 + \frac{k_1}{k_2[A]} e^{(k_1+k_2[A]_0)t}} \quad (1)$$

This formula then correlates with the iodobenzene (PhI) concentration as $[PhI]_t = 500[A]_t$ since the total amount of Pd precatalyst is 0.2 mol % ($=500^{-1}$). Figure 4 shows the concentration of iodobenzene in time for several precatalysts (data points markers), while the solid lines represent the calculated values of $500[A]_t$ for each precatalyst according to

(43) Parshall, G. W. *J. Am. Chem. Soc.* **1974**, *96* (8), 2360–2366.

(44) Gouterman, M. In *The Porphyrins*; Dolphin, D., Ed.; Academic Press, Inc.: New York, 1978; Vol. 3.

(45) Widegren, J. A.; Aiken, I. J. D.; Özkaz, S.; Finke, R. G. *Chem. Mater.* **2001**, *13*, 312–324.

(46) Watzky, M. A.; Finke, R. G. *J. Am. Chem. Soc.* **1997**, *119*, 10382–10400.

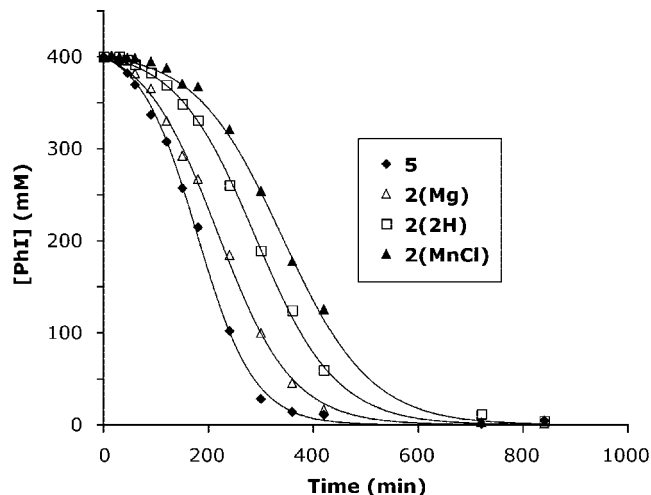


Figure 4. Graph representing the decrease in PhI concentration in time (data points) and the fitted values for $500[A]_t$ (black lines). The data for **2(Ni)** are not shown due to poor fit results.

Table 2. Fitted Kinetic Data for Reaction 1 According to Eq 1

	k_1 ($\times 10^{-6} \text{ min}^{-1}$)	k_2 ($\text{M}^{-1} \text{ min}^{-1}$)
5	675 ± 60	22.1 ± 0.9
2(Mg)	638 ± 92	16.7 ± 1.2
2(2H)	293 ± 30	15.9 ± 0.6
2(MnCl)	238 ± 81	13.5 ± 1.7

eq 1. The fit results for **5**, **2(Mg)**, **2(2H)**, and **2(MnCl)** are relatively accurate, which is a strong indication for the plausibility of the Finke model for the current systems.⁴⁷ Only at longer reaction times does the model not accurately fit the experimental data. The fitted values for k_1 and k_2 are listed in Table 2. The catalytic data of the nickel complex could not be fitted to the model.

According to these values, the ease of generation of the true catalysts from the pincer-porphyrin hybrids seems to correlate to the electron density on the (metallo)porphyrin. An increase in the electron-donating ability of the porphyrin (**2(MnCl)** < **2(2H)** < **2(Mg)**) leads to an increase of both k_1 and k_2 , which means that it enhances the rate of Pd(0) formation as well as the rate of the autocatalytic reaction. On the other hand, none of the **2(M)** hybrids exceeds the reactivity of parent compound **5**.

UV/Vis during Catalysis. During the course of the Heck reactions, the electronic spectra of the catalysis mixtures of **2(2H)**, **2(Mg)**, and **2(Ni)** did not undergo substantial changes. The intensity ratios between the Soret and Q-band(s) and their appearance remained identical throughout the course of the reaction, which indicates that demetalation of **2(Ni)** and, more notably, of **2(Mg)** did not occur. However, it was noted that the Soret bands of **2(2H)**, **2(Mg)**, and **2(Ni)** gradually shifted to shorter wavelengths by ~ 6 nm (see Figure 5 for **2(2H)**). In fact, the wavelengths at which the Soret and Q-bands resided at the end of the reactions coincide with those of the corresponding **1(M)** parent compounds, which corroborates leaching of Pd from the SCS-pincer moieties.

The UV/vis spectrum of **2(MnCl)** did, on the other hand, show significant changes during the catalytic run. A Soret-type band around 445 nm with Q-bands at 529, 577, and 620 nm

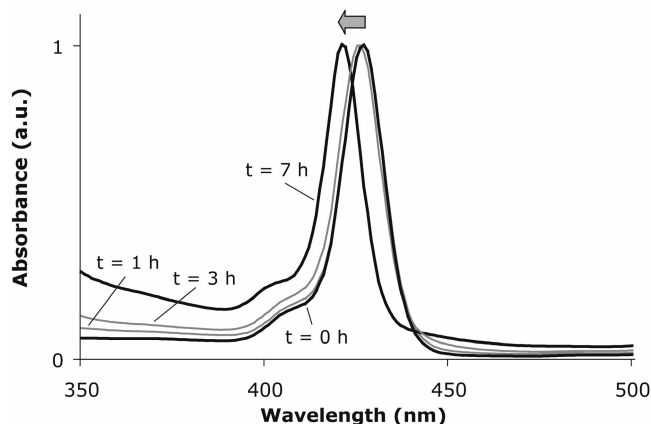


Figure 5. Evolution of the normalized Soret band area of **2(2H)** during reaction 1.

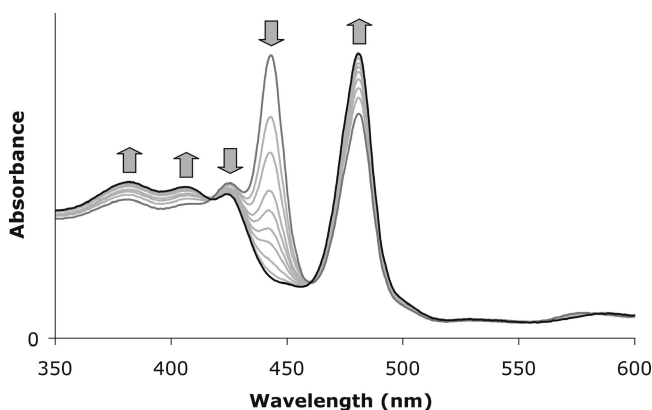


Figure 6. Reaction of a sample taken from the **2(MnCl)**-catalyzed Heck reaction with air.

increased in intensity at the expense of the Soret band of **2(MnCl)** at 481 nm. The new bands are similar to the absorption bands observed for nitrogenous base adducts of Mn(II) tetrakis(aryl)porphyrins ($\sim 440, 532, 575, 613$ nm in THF).^{48,49} When a sample in CH_2Cl_2 , taken 60 min after initiation of the reaction, was exposed to air, the 481 nm Mn(III) porphyrin band increased again with clear isosbestic points, indicating a conversion from one species into the other (Figure 6). As the Heck reaction continued, the 445 nm band decreased again at the benefit of broad bands between 500 and 750 nm, which could not be compared to literature values for discrete manganese porphyrins. Independent experiments on **6(MnCl)** showed a similar behavior of the electronic spectra under the catalytic conditions. Further investigations showed that the sole addition of Et_3N to a solution of **6(MnCl)** in DMF (119°C) caused virtually identical spectral changes. Hence, these spectral changes are not brought about by the merger of the SCS-pincer PdCl groups with the manganese tetraphenylporphyrin skeleton, but by a reduction of the manganese porphyrin by Et_3N .

During the Heck reaction catalyzed by the parent SCS-pincer palladium(II) complex **5** the UV/vis spectra showed a new, gradually increasing absorption band around 440 nm. The position of this band agrees excellently with the data obtained by Dupont et al. for their κ^2 -C,N-palladacycle and was attributed

(47) Although the fits do closely resemble the experimental data, it should be noted that this cannot be taken as conclusive proof for the stated model of catalysis by palladium leaching, as was argued by Weck (ref 17).

(48) Jones, R. D.; Summerville, D. A.; Basolo, F. *J. Am. Chem. Soc.* **1978**, *100* (14), 4416–4424.

(49) Reed, C. A.; Kouba, J. K.; Grimes, C. J.; Cheung, S. K. *Inorg. Chem.* **1978**, *17* (9), 2666–2670.

to the formation of PdX_n^- species ($X = \text{halide}$).^{50,51} The Soret regions of **2(M)** coincide with the diagnostic region for these PdX_n^- salts and, therefore, prevented their possible observation. The formation of Pd nanoparticles was, however, strongly indicated by the considerable darkening of the reaction mixtures and by very broad absorptions at longer wavelengths.

Discussion

Palladacyclic compounds in general and ECE-pincer PdCl complexes in particular have been widely applied as precatalysts for Heck reactions. They are able to activate aryl chlorides and show impressive turnover numbers without significant deposition of palladium black.^{13,15–17,19,20,37,52–55} It was speculated that such palladacycles exhibit exceedingly high activities due to their ability to stabilize tetravalent palladium intermediates involved in a Pd(II)/Pd(IV) catalytic mechanism.^{37,56} Recently, Bergbreiter,¹⁵ Weck and Jones,^{16,17} and Eberhard⁵⁷ showed convincingly that SCS- and PCP-pincer PdCl complexes are not the actual catalysts for high-temperature palladium-catalyzed Heck reactions between aryl halides and activated terminal olefins, but rather are catalyst precursors. They showed that these palladacyclic complexes slowly release Pd(0) particles that subsequently take part in catalysis via a Pd(0)/Pd(II) mechanism. Although these results have disproved the originally proposed Pd(II)/Pd(IV) molecular mechanism,^{15–17,37,58} (ECE-type) palladacycles are still being extensively used as precatalysts because of the high turnover numbers (TON) that can be obtained.^{14–17} It was recently very convincingly put forward by De Vries that the Pd(0)/Pd(II) mechanism is in fact operable in all high-temperature Heck reactions.⁵⁸

The tetrakis(SCS-pincer PdCl)–(metallo)porphyrin hybrid systems described here also gradually eliminate Pd particles when used in a Heck reaction. Evidence for this process was provided by the putative formation of the parent **1(M)** systems from the peripherally palladated **2(M)** species during the course of the reaction, as observed by UV/vis spectroscopy.

The nature of the (metallo)porphyrin part within the pincer–porphyrin hybrids **2(M)** seems to have a considerable effect on the rate of the Heck reaction between iodobenzene and styrene. Combinations of **6(M)** and **5** did not lead to altered activities in the same reaction and, hence, the differences between the performances of the pincer–porphyrin hybrids as catalyst precursors originate from intramolecular effects. It was also observed that the electronic properties of free-base, magnesium(II), nickel(II), and zinc(II) porphyrins are passed on to peripheral NCN-pincer Pt(II) centers.^{32,33} Although direct means to probe the electron density at the palladium centers of the **2(M)** porphyrins were not employed, the similarities between SCS- and NCN-pincer metal systems suggest that also in the SCS-pincer Pd complexes discussed here the electronic proper-

ties of the (metallo)porphyrin influence the peripheral Pd centers in a similar manner. For the related NCN-pincer complexes of Ni,²⁸ Pd,²⁵ and Pt^{26,27} and other pincer complexes^{29,30} it is known that changes in the electronic parameters of their *para*-substituents lead to changes in for example the redox potential²⁸ or NMR chemical shift²⁶ of the ligated metal center. For these reasons, the Pd sites in the current systems are anticipated to be influenced as well; that is, electronic variations on the (metallo)porphyrin are passed on to the peripheral SCS-pincer palladium centers. During the preparation of this article, an interesting report by Osuka et al. appeared in which they used metalloporphyrins in a similar way to modulate the catalytic properties of a bis(2-pyridyl)pincer palladium complex in a Heck reaction.⁵⁹

Bergbreiter et al. recently showed that the kinetics of a similar Heck reaction, catalyzed by 3,5-[(4-*X*-phenylsulfido)methyl]-4-(pseudo)halidopalladio(II) acetanilides ($X = \text{H, NMe}_2, \text{NHC}(\text{O})\text{Me, OMe, COOH}$), did not depend on the thiophenyl *para*-substituent *X*. This can be rationalized by the fact that, during the decomposition pathway, the sulfur atoms are displaced from the palladium center by triethylamine, prior to the steps culminating in palladium leaching.¹⁷ Weck, on the other hand, mentioned that all reactions leading to palladium(0) formation after decoordination of the sulfide groups are thermodynamically downhill,¹⁶ which seems to contradict the finding of Bergbreiter in that no correlation was found between the strength of the Pd–S bond, which is expected to depend on *X*, and the catalytic activity of the system. In the investigations presented here, modification of an SCS-pincer PdCl moiety at the position *para* with respect to the carbon–palladium bond was found to have considerable effects on its catalytic properties in a Heck reaction. It therefore seems that the strength of the Pd–C bond in SCS-pincer Pd complexes does have an effect on the overall stability of these complexes and, consequently, on their activity in Heck catalysis, as opposed to the strength of the Pd–S bond.

On the basis of the calculated *k* values it seems that both *k*₁ and *k*₂ become larger as the metalloporphyrin becomes a better electron donor. This indicates that the release of Pd from SCS-pincer PdCl complexes and the following autocatalytic process are both enhanced by an electron-rich *para*-substituent. It was noted that for **2(MnCl)** the fit of the experimental data to the Finke model is poor at longer reaction times, which is probably caused by secondary processes. In this regard it should be noted that free-base, nickel(II), and magnesium(II) porphyrins are not considered to be redox-active at the metal, whereas manganese(III) porphyrins are susceptible to both reductive and oxidative changes. The profound changes we observed in the electronic spectra of the catalytic mixture of **2(MnCl)** support the assumption that several different manganese porphyrins are present in the reaction mixture at any given moment. Therefore, an exact description of the manganese porphyrin species responsible for palladium leaching is not straightforward.

The parent SCS-pincer palladium complex **5** is the most active compound among all investigated precatalysts. We have also noted that the attachment of a free-base, nickel, or zinc porphyrin to the *para*-position of a related NCN-pincer platinum complex led to a higher platinum-centered electron density compared to its *para*-H analogue.³² Although this might suggest that also in **5** the electron density on palladium is lower than in the free-base, magnesium, and nickel complexes **2(2H)**, **2(Mg)**, and **2(Ni)**, this does not take into account that the leaching process at one site in a pincer–porphyrin hybrid precatalyst may

(50) Consorti, C. S.; Flores, F. R.; Dupont, J. *J. Am. Chem. Soc.* **2005**, *127*, 12054–12065.

(51) Dupont, J.; Basso, N. R.; Meneghetti, M. R.; Konrath, R. A.; Burrow, R.; Horner, M. *Organometallics* **1997**, *16*, 2386–2391.

(52) Soro, B.; Stoccoro, S.; Minghetti, G.; Zucca, A.; Cinellu, M. A.; Manassero, M.; Gladiali, S. *Inorg. Chim. Acta* **2006**, *359*, 1879–1888.

(53) Takenaka, K.; Uozumi, Y. *Adv. Synth. Catal.* **2004**, *346*, 1693–1696.

(54) Yoon, M. S.; Ryu, D.; Kim, J.; Ahn, K. H. *Organometallics* **2006**, *25*, 2409–2411.

(55) Ogo, S.; Takebe, Y.; Uehara, K.; Yamazaki, T.; Nakai, H.; Watanabe, Y.; Fukuzumi, S. *Organometallics* **2006**, *25*, 331–338.

(56) Herrmann, W. A.; Böhm, V. P. W.; Reisinger, C.-P. *J. Organomet. Chem.* **1999**, *576*, 23–41.

(57) Eberhard, M. R. *Org. Lett.* **2004**, *6* (13), 2125–2128.

(58) de Vries, J. G. *Dalton Trans.* **2006**, 421–429.

(59) Yamaguchi, S.; Katoh, T.; Shinokubo, H.; Osuka, A. *J. Am. Chem. Soc.* **2007**, *129*, 6392–6393.

influence the leaching of palladium at another SCS-pincer site within the same molecule. In other words, the intramolecular effects of palladium leaching may lead to an overall retardation of the leaching process. Simultaneously, another factor of importance in this regard may be the high local concentration of Pd(0) around a molecule of **2(M)** once it has leached a palladium atom, which concomitantly affects the equilibria leading to palladium leaching by the other metalated pincer sites.

Conclusions

A number of *meso*-tetrakis(SCS-pincer PdCl)–metalloporphyrin hybrids have been synthesized in high yields using orthogonal metalation procedures for either ligand site. Upon use of these compounds in the Heck reaction of iodobenzene with styrene, they show a marked difference in activity. The Mn(III) porphyrin precatalyst exhibited the lowest activity while the Mg(II) porphyrin precatalyst showed the highest activity. As these observations are in line with the relative electron-donating properties of the (metallo)porphyrin moieties, they show that the nature of the porphyrin has a direct influence on the (catalytic) properties of its peripheral Pd-moieties. Although this proof-of-principle study did not lead to the development of (pre)catalysts with increased activities compared to their SCS-pincer PdCl congener, it does bear out the usefulness of metalloporphyrins as catalyst-modulating substituents, which was the objective of this study.

Experimental Section

General Comments. All reactions were performed under a nitrogen atmosphere using standard Schlenk techniques. All reactions involving porphyrin compounds were shielded from ambient light using aluminum foil. Et₂O and THF were carefully dried and distilled from sodium/benzophenone prior to use. CH₂Cl₂, MeCN, *N,N*-dimethylformamide (DMF), *N,N*-diisopropylethylamine, and triethylamine were distilled from CaH₂. Iodobenzene and styrene were distilled at low pressures prior to use and stored at –30 °C. Just before use, all solvents were deoxygenated by bubbling a steady stream of dry nitrogen through them while stirring vigorously for at least 20 min. **1(2H)** was obtained as described before,³¹ and [Pd(NCMe)₄](BF₄)₂ was synthesized from Pd(0) and NOBF₄ in MeCN according to a published procedure.⁶⁰ Column chromatography was performed using ACROS silica gel for column chromatography, 0.060–0.200 mm, pore diameter ca. 6 nm, or Merck aluminum oxide 90 active basic (0.063–0.200 mm). ¹H and ¹³C{¹H} NMR spectra were recorded at 300 and 75 MHz, respectively, on a Varian 300 spectrometer operating at 298 K and were referenced to the residual solvent signal. UV/vis spectra were recorded on a Cary 50 scan UV–visible spectrophotometer. Chromatographic analysis of the catalysis mixtures was carried out on a Perkin-Elmer AutoSystem XL gas chromatograph. MALDI-TOF measurements were performed on an Applied Biosystems Voyager-DE PRO biospectrometry workstation with 2,5-dihydroxybenzoic acid (DHB) or 9-nitroanthracene (9NA) or without matrix (LDI). ESI-MS measurements were performed at the Biomolecular Mass Spectrometry Group, Bijvoet Centre for Biomolecular Research, Utrecht University, The Netherlands. Elemental microanalyses were performed by Dornis und Kolbe, Mikroanalytisches Laboratorium, Müllheim a/d Ruhr, Germany.

[5,10,15,20-Tetrakis(3,5-bis[(4-*tert*-butylphenylsulfido)methyl]phenyl)porphyrinato)manganese(III) Chloride (1(MnCl)). To a dark red solution of **1(2H)** (45.0 mg, 22 μmol) in degassed, dry DMF (5 mL) was added Mn(OAc)₂·4H₂O (200 mg, 816 μmol) at once, and the solution was heated to reflux for 16 h under nitrogen.

The brownish mixture was allowed to reach room temperature (RT) and was evaporated to dryness in vacuo. The remaining solid was dissolved in CHCl₃ (35 mL), air was bubbled through the solution for 30 s (in the dark), brine (35 mL) was added, and the biphasic system was vigorously stirred for 5 min at room temperature. The organic layer was separated, dried (MgSO₄), filtered, and evaporated to leave a green solid. The solid was purified by dry column chromatography (basic alumina), eluting with CHCl₃ and subsequently with 3% MeOH in CHCl₃ to elute the desired product. Finally, the compound was recrystallized from hexane at –30 °C. Yield: 40.8 mg (87%). IR (cm^{–1}): 3074, 2957, 2865, 1595, 1488, 1459, 1394, 1361, 1347, 1268, 1227, 1205, 1120, 1062, 1012, 946, 897, 819, 803, 742, 713. UV/vis [λ_{\max} (log ϵ), CH₂Cl₂]: 376 (4.66), 402 (4.66), 422 (4.60), 479 (5.14), 540 (3.77), 585 (4.00), 620 (4.12) nm. MALDI-TOF MS (DHB): *m/z* 2091.51 ([M – Cl]⁺), calcd for C₁₃₂H₁₄₀MnN₄S₈: 2091.81; 1928.50 ([M – Cl – *tert*-BuPhS·]⁺), calcd for C₁₂₂H₁₂₇MnN₄S₇: 1928.78. Anal. Calcd for C₁₃₂H₁₄₀ClMnN₄S₈: C 74.45, H 6.63, N 2.63, S 12.05. Found: C 74.32, H 6.51, N 2.78, S 11.88.

[5,10,15,20-Tetrakis(3,5-bis[(4-*tert*-butylphenylsulfido)methyl]-4-chloridopalladio(II)-phenyl)porphyrinato)manganese(III) Chloride (2(MnCl)). A green solution of **1(MnCl)** (21.1 mg, 9.91 μmol) in a CH₂Cl₂/MeCN mixture (8 mL/4 mL) was treated with a solution of [Pd(NCMe)₄](BF₄)₂ (17.6 mg, 39.8 μmol) in MeCN (4 mL), whereupon the solution immediately turned dark orange. After 5 h of stirring at room temperature, the mixture was heated to 45 °C for 16 h. After cooling to room temperature, triethylamine (5 drops) was added and the green solution was stirred for an additional hour and evaporated to dryness. The green solid was then redissolved in MeCN (60 mL) and treated with LiCl (excess) while stirring to give a voluminous green precipitate. After 2 h, the precipitate was isolated by centrifugation and partitioned between CH₂Cl₂ (20 mL) and H₂O (50 mL). The organic layer was isolated, dried (MgSO₄), filtered, and concentrated to 10 mL. Upon addition of pentane (80 mL), the product precipitated as a green solid, which was washed with Et₂O (80 mL) and redissolved in CH₂Cl₂ and filtered over a plug of silica gel (eluent: 3% MeOH in CH₂Cl₂). The fast running, first green band was collected, concentrated to 10 mL and Et₂O was added to precipitate the product as a green solid, which was isolated by centrifugation and dried in vacuo. Yield: 23.0 mg (86%). IR (cm^{–1}): 3478 (br), 3049, 2959, 2867, 1593, 1488, 1460, 1397, 1363, 1346, 1268, 1204, 1116, 1081, 1062, 1011, 946, 904, 818, 804, 714. UV/vis [λ_{\max} (log ϵ), CH₂Cl₂]: 338 (4.79), 381 (4.84), 407 (4.83), 424 (4.80), 481 (5.20), 531 (3.89), 588 (4.09), 624 (4.25) nm. MALDI-TOF MS (9NA): *m/z* 2690.58 ([M]⁺), calcd for C₁₃₂H₁₃₆Cl₅MnN₄Pd₄S₈: 2690.26; 2656.00 ([M – Cl]⁺), calcd for C₁₃₂H₁₃₆Cl₄MnN₄Pd₄S₈: 2655.29; 2548.54 ([M – PdCl]⁺), calcd for C₁₃₂H₁₃₆Cl₃MnN₄Pd₃S₈: 2548.38; 2406.58 ([M – 2(PdCl)]⁺), calcd for C₁₃₂H₁₃₆Cl₂MnN₄Pd₂S₈: 2406.51; 2264.83 ([M – 3(PdCl)]⁺), calcd for C₁₃₂H₁₃₆ClMnN₄PdS₈: 2264.63; 2123.32 ([M – 4(PdCl)]⁺), calcd for C₁₃₂H₁₃₆ClMnN₄S₈: 2122.76. Anal. Calcd for C₁₃₂H₁₃₆Cl₅MnN₄Pd₄S₈: C 58.87, H 5.09, N 2.08, S 9.53. Found: C 58.93, H 5.04, N 2.12, S 9.46.

[5,10,15,20-Tetrakis(3,5-bis[(4-*tert*-butylphenylsulfido)methyl]phenyl)porphyrinato]nickel(II) (1(Ni)). To a dark red solution of **1(2H)** (150 mg, 73.5 μmol) in dry, degassed toluene (30 mL) was added Ni(acac)₂ (0.38 g, 1.47 mmol), and the mixture was heated to reflux. The reaction progress was monitored by UV/vis spectroscopy in dry CH₂Cl₂ and after 2 h, the lowest energy Q-band (645 nm) of **1(2H)** had disappeared. The volatiles were subsequently evaporated in vacuo, and the resulting red solid was dissolved in CH₂Cl₂ (30 mL) and washed with H₂O (60 mL) and brine (60 mL). The organic layer was dried (MgSO₄), filtered, and concentrated to 5 mL. EtOH (80 mL) was added, and after concentration of the mixture to ~30 mL, the red product was isolated by centrifugation and dried in vacuo. Yield: 151 mg (98%). ¹H NMR (CDCl₃): δ 8.54 (s, 8H, β H), 7.66 (s, 8H, ArH), 7.59 (s, 4H, ArH), 7.32 (d,

(60) Yuan, J.-C.; Lu, S.-J. *Organometallics* **2001**, *20*, 2697–2703.

$^3J_{\text{HH}} = 8.4$ Hz, 16H, ArH), 7.24 (d, $^3J_{\text{HH}} = 8.4$ Hz, 16H, ArH), 4.24 (s, 16H, CH_2S), 1.13 (s, 72H, $\text{C}(\text{CH}_3)_3$) ppm. $^{13}\text{C}\{^1\text{H}\}$ NMR (CDCl_3): δ 150.2, 142.6, 141.0, 136.8, 133.1, 132.2, 131.1, 129.1, 126.1, 118.5, 39.9, 34.5, 31.2 ppm. UV/vis [λ_{max} (log ϵ), CH_2Cl_2]: 417 (5.43), 527 (4.30) nm. ESI-MS: m/z 2094.80 ($[\text{M} + \text{H}]^+$), calcd for $\text{C}_{132}\text{H}_{141}\text{N}_4\text{NiS}_8$: 2094.82. Anal. Calcd for $\text{C}_{132}\text{H}_{140}\text{N}_4\text{NiS}_8$: C 75.57, H 7.28, N 2.56, S 11.72. Found: C 75.64, H 7.28, N 2.51, S 11.58.

[5,10,15,20-Tetrakis(3,5-bis[(4-*tert*-butylphenylsulfido)methyl]-4-chloridopalladio(II)phenyl)porphyrinato]nickel(II) (2(Ni)). Compound **1(Ni)** (134 mg, 64 μmol) was dissolved in dry CH_2Cl_2 (30 mL), and the bright red solution was diluted with MeCN (30 mL) and stirred at room temperature. $[(\text{Pd}(\text{NCMe})_4)(\text{BF}_4)_4]$ (142 mg, 330 μmol) dissolved in MeCN (5 mL) was added, and the red solution was stirred at reflux temperature overnight. All volatiles were subsequently evaporated, and the resulting orange plaque was dissolved in MeCN (30 mL). A large excess of LiCl was added, and the resulting suspension was stirred for an additional hour. The solids were isolated by means of centrifugation and stirred in a biphasic system of CH_2Cl_2 (20 mL) and H_2O (40 mL). After 30 min the organic layer was isolated, dried (MgSO_4), and filtered. The solution was concentrated to 10 mL, and hexanes (50 mL) were added to induce precipitation of the product as an orange solid. Yield: 152 mg (89%). ^1H NMR (CDCl_3): δ 8.73 (s, 8H, βH), 7.91 (d, $^3J_{\text{HH}} = 8.4$ Hz, 16H, ArH), 7.57 (s, 8H, ArH), 7.47 (d, $^3J_{\text{HH}} = 8.4$ Hz, 16H, ArH), 4.77 (br s, 16H, CH_2S), 1.34 (s, 72H, $\text{C}(\text{CH}_3)_3$) ppm. $^{13}\text{C}\{^1\text{H}\}$ NMR (CDCl_3): δ 160.7, 153.6, 148.1, 142.8, 137.5, 132.2, 131.8, 129.0, 127.4, 127.0, 118.5, 53.0, 35.1, 31.4 ppm. UV/vis [λ_{max} (log ϵ), CH_2Cl_2]: 422 (5.85), 531 (4.73) nm. MALDI-TOF MS (9NA): m/z 2623.80 ($[\text{M} - \text{Cl}]^+$), calcd for $\text{C}_{132}\text{H}_{136}\text{Cl}_3\text{N}_4\text{NiPd}_4\text{S}_8$: 2623.32. Anal. Calcd for $\text{C}_{132}\text{H}_{136}\text{Cl}_4\text{N}_4\text{NiPd}_4\text{S}_8$: C 59.58, H 5.15, N 2.11, Ni 2.21, S 9.64. Found: C 59.63, H 5.19, N 2.19, Ni 2.26, S 9.59.

[5,10,15,20-Tetrakis(3,5-bis[(4-*tert*-butylphenylsulfido)methyl]-4-chloridopalladio(II)phenyl)porphyrinato]magnesium(II) (2(Mg)). Dry Et_3N (68 μL , 490 μmol) was added to a stirred, dark red solution of **2(2H)** (32 mg, 12 μmol) in dry CH_2Cl_2 (4 mL). After 5 min, $\text{MgBr}_2 \cdot \text{OEt}_2$ (64 mg, 246 μmol) was added at once, and the solution was stirred at room temperature. The progress of the reaction was monitored by UV/vis spectroscopy, which showed the disappearance of the lowest energy free-base porphyrin band at 650 nm upon metalation with magnesium. After 1 h, all volatiles were evaporated in vacuo. The residue was taken up in CH_2Cl_2 (5 mL) and filtered over a short pad of basic Al_2O_3 , which was first

eluted with CH_2Cl_2 (50 mL) and then with 5% MeOH in CH_2Cl_2 to elute the product as a purple-pink band. The volatiles were removed, the residue was redissolved in CH_2Cl_2 , and hexanes (40 mL) were added to induce precipitation of the product as a green solid. Yield: 29 mg (90%). ^1H NMR ($\text{CDCl}_3/1\%$ pyridine- d_5): δ 8.87 (s, 8H, $\beta\text{-H}$), 7.94 (d, $^3J_{\text{HH}} = 8.4$ Hz, 16H, ArH), 7.80 (s, 8H, ArH), 7.49 (d, $^3J_{\text{HH}} = 8.4$ Hz, 16H, ArH), 4.85 (br s, 16H, CH_2S), 1.35 (s, 72H, $\text{C}(\text{CH}_3)_3$) ppm. $^{13}\text{C}\{^1\text{H}\}$ NMR ($\text{CDCl}_3/1\%$ pyridine- d_5): δ 163.3, 153.8, 150.1, 147.6, 140.6, 132.0, 132.0, 129.4, 128.5, 127.0, 121.2, 53.8, 35.1, 31.4 ppm. UV/vis [λ_{max} (log ϵ), CH_2Cl_2]: 314 (4.62), 413 (4.79), 433 (5.82), 528 (3.75), 567 (4.35), 609 (4.27) nm. MALDI-TOF MS (9NA): m/z 2726.36 ($[\text{M} + \text{Et}_3\text{N}]^+$), calcd for $\text{C}_{138}\text{H}_{151}\text{Cl}_4\text{MgN}_5\text{Pd}_4\text{S}_8$: 2725.46. Anal. Calcd for $\text{C}_{132}\text{H}_{136}\text{Cl}_4\text{MgN}_4\text{Pd}_4\text{S}_8$: C 60.35, H 5.22, N 2.13, S 9.77. Found: C 60.26, H 5.18, N 2.20, S 9.63.

General Procedure for the Heck Reaction. A flame-dried Schlenk tube was charged with DMF (7.89 mL), pentadecane (550 μL , 2.00 mmol), freshly distilled iodobenzene (448 μL , 4.00 mmol), styrene (687 μL , 6.00 mmol), and triethylamine (836 μL , 6.00 mmol), and the solution (total volume: 10.0 mL) was heated to 119 $^\circ\text{C}$. In a separate vial, the respective precatalyst (2.00 μmol **2(M)**; 8.00 μmol [Pd] or a mixture of 8.00 μmol of **5** and 2.00 μmol of **6(M)**) was weighed accurately, and the preheated substrate solution was subsequently added at once via syringe ($t = 0$). The solution was immediately immersed in a preheated (119 $^\circ\text{C}$) carousel reactor and magnetically stirred at 800 rpm under air. The reactions were shielded from ambient light with aluminum foil. Samples (~ 30 μL) for substrate/product analysis were taken at regular time intervals and diluted in a GC vial with Et_2O (~ 1.5 mL). Samples for UV/vis measurements (~ 20 μL) were diluted in a cuvette containing dry, deoxygenated CH_2Cl_2 (3.0 mL), and the sample was immediately measured.

Acknowledgment. We thank The Netherlands Organisation for Scientific Research for a Jonge Chemici scholarship (B.M.J.M.S. and R.J.M.K.G.) and for an Erasmus stipend (S.D.H.M.).

Supporting Information Available: Experimental procedures for the preparation of compounds **5** and **6(M)** as well as a reproduction of the X-ray crystal structure of **2(2H)** are available free of charge via the Internet at <http://pubs.acs.org>.

OM7005613